

# High Selectivity for Ethylene from Carbon Dioxide Reduction over Copper Nanocube Electrocatalysts\*\*

F. Sloan Roberts, Kendra P. Kuhl, and Anders Nilsson\*

**Abstract:** Nanostructured surfaces have been shown to greatly enhance the activity and selectivity of many different catalysts. Here we report a nanostructured copper surface that gives high selectivity for ethylene formation from electrocatalytic  $\text{CO}_2$  reduction. The nanostructured copper is easily formed in situ during the  $\text{CO}_2$  reduction reaction, and scanning electron microscopy (SEM) shows the surface to be dominated by cubic structures. Using online electrochemical mass spectrometry (OLEMS), the onset potentials and relative selectivity toward the volatile products (ethylene and methane) were measured for several different copper surfaces and single crystals, relating the cubic shape of the copper surface to the greatly enhanced ethylene selectivity. The ability of the cubic nanostructure to so strongly favor multicarbon product formation from  $\text{CO}_2$  reduction, and in particular ethylene over methane, is unique to this surface and is an important step toward developing a catalyst that has exclusive selectivity for multicarbon products.

A promising path to reducing carbon dioxide emissions into the atmosphere is recycling carbon dioxide into fuels and commodity chemicals through an electrochemical process.<sup>[1]</sup> Electrocatalyst development for the carbon dioxide reduction reaction ( $\text{CO}_2\text{RR}$ ) is key to enabling the widespread adoption of this technology. Many studies have focused on copper metal as a catalyst, because it is known to produce a mixture of methane and ethylene and other minor products (Table S1).<sup>[2]</sup> However, improvements in energy efficiency, achieved by lowering the overpotential of the  $\text{CO}_2\text{RR}$ , and in selectivity, by increasing the yield of the desired product, are needed.

Recent work has shown that modifying the structure of the copper surface is a path to better efficiency and selectivity. Oxidizing and then reducing copper metal leads to a highly nanostructured surface, with much lower overpotential (higher energy efficiency) for the  $\text{CO}_2\text{RR}$ .<sup>[3]</sup> Other work has compared the activity of single-crystal faces and found that

although most surfaces have similar activity for methane and ethylene, the Cu(100) surface favors ethylene formation at a lower overpotential compared to methane.<sup>[4]</sup> In an effort to produce higher surface area catalysts with a large amount of exposed (100) facets, there has been an interest in copper nanocubes as catalysts for  $\text{CO}_2\text{RR}$  with higher selectivity for ethylene and better energy efficiency than unstructured polycrystalline copper.<sup>[5]</sup>

Increasing the selectivity of copper for ethylene over methane is desirable as ethylene is a popular chemical commodity used in industrial applications, and there is abundant and cheap access to methane via natural gas. Ethylene selectivity also has broader implications in the field of  $\text{CO}_2\text{RR}$  catalysis, because it provides insight into the C–C coupling reaction step that must occur for the formation of multicarbon products. Understanding and controlling this step is of paramount importance to guide the design of catalysts with high selectivity for the desired product. Herein, we report a simple in situ synthesis of a nanocube-covered copper (CuCube) surface with high selectivity and low overpotential for ethylene formation, adding to evidence that (100) sites are highly active for C–C coupling and can lead to developing strategies to target multicarbon products.

Successive oxidative–reductive cycles in the presence of KCl changes the surface structure of the starting polycrystalline copper into the CuCube surface (Figure 1 A), composed of monolithic structures made up of predominantly cubic faces, in contrast to the copper surface cycled without chloride ions (Figure 1 B), which has few distinct features. The addition of KCl likely promotes the formation of the CuCube structure through the initial formation of CuCl under oxidizing conditions.<sup>[6]</sup> CuCl is known to form cubes when it precipitates in solutions above pH 4.<sup>[7]</sup> In the presence of water, CuCl can convert to  $\text{Cu}_2\text{O}$  through an equilibrium reaction which favors copper oxide formation in neutral and basic solutions with low chloride concentrations,<sup>[6,7]</sup> as present in this experiment. XPS of CuCube surfaces removed from solution at oxidative potentials show that only trace amounts of Cl are present (Figure S5), suggesting that CuCl formed at these oxidative potentials has been converted to  $\text{Cu}_2\text{O}$ . XRD (Figure S4), which probes the bulk rather than the surface, shows that only copper and  $\text{Cu}_2\text{O}$  phases are detected in the CuCube sample. These results support the mechanism of CuCube formation described above, in which CuCl formation and precipitation is responsible for the cubic shape, but is then converted to  $\text{Cu}_2\text{O}$ . It is worth mentioning that the  $\text{Cu}_2\text{O}$  surface is subsequently reduced before the  $\text{CO}_2\text{RR}$  begins, leaving metallic copper (now in a cubic structure) as the active catalytic surface.

[\*] Dr. F. S. Roberts,<sup>[‡]</sup> Dr. K. P. Kuhl,<sup>[‡]</sup> Prof. A. Nilsson  
Department of Chemistry, Stanford University  
Stanford, CA 94305 (USA)  
E-mail: nilsson@slac.stanford.edu

[‡] These authors contributed equally to this work.

[\*\*] This work is supported by Air Force Office of Scientific Research through the MURI program under AFOSR Award No. FA9550-10-1-0572 and the Global Climate Energy Project at Stanford University. The XPS, XRD, and SEM studies were performed at the Stanford Nano Center (SNC)/Stanford Nanocharacterization Laboratory (SNL) part of the Stanford Nano Shared Facilities.



Supporting information for this article is available on the WWW under <http://dx.doi.org/10.1002/anie.201412214>.

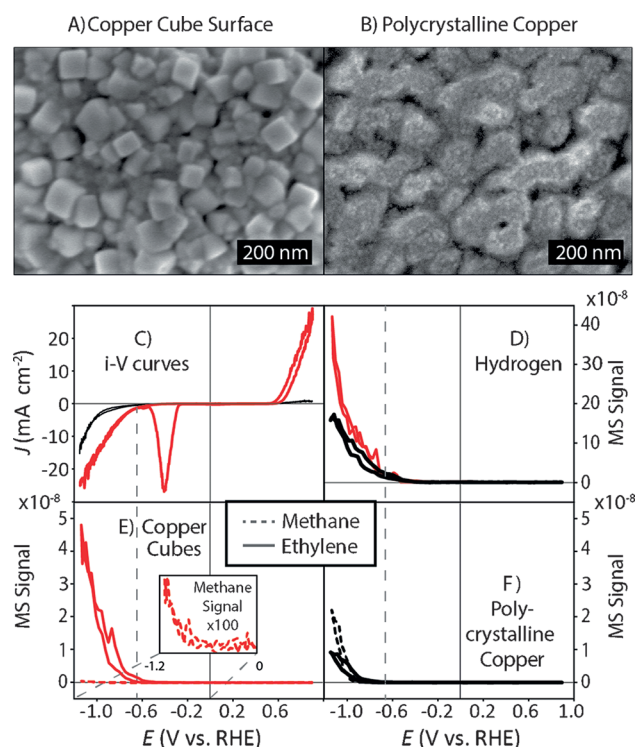


**Figure 1.** SEM images of A) the CuCube surface formed by cycling a polycrystalline electrode between  $-1.15$  and  $0.9$  V three times with  $4$  mM KCl in  $0.1$  M KHCO<sub>3</sub> and B) a polycrystalline copper electrode after cycling in the same voltage region three times without KCl in  $0.1$  M KHCO<sub>3</sub>. C) Cyclic voltammograms of CuCube (red) and polycrystalline (black) copper surfaces and corresponding hydrogen formation measured by OLEMS shown in (D). Methane (dashed) and ethylene (solid) formation measured by OLEMS on E) the CuCube surface and F) polycrystalline copper, showing a dramatic shift in selectivity toward ethylene and away from methane.

Figure 1C shows the CVs of a polycrystalline copper electrode in aqueous  $0.1$  M KHCO<sub>3</sub> without (black) and with (red) the addition of  $4$  mM KCl. The addition of KCl leads to significant changes in the CV. At oxidative potentials ( $0.5$  to  $0.9$  V vs. RHE) orders of magnitude more current is drawn when chloride ions are present and the oxidized copper that is formed at high potentials is reduced in the large negative peak between  $-0.2$  and  $-0.5$  V. Going to voltages lower than  $-0.5$  V, the CuCube sample (red), formed by successive oxidative–reductive scans in the presence of KCl, draws more current than polycrystalline copper without the addition of KCl. The higher current density drawn by the CuCube sample negative of  $-0.5$  V is likely due to the higher surface roughness of the nanostructured surface compared to the electropolished polycrystalline Cu surface (see the Supporting Information, SI).

Measurements of the products formed from the CO<sub>2</sub>RR (and competing water reduction to hydrogen) were made using an OLEMS system (see the Experimental Section and SI for a detailed description). The data for polycrystalline copper (black) are consistent with reported results.<sup>[2a]</sup> Polycrystalline copper has an early onset for hydrogen production compared to any CO<sub>2</sub>RR products. Methane and ethylene, CO<sub>2</sub>RR products, have onsets around  $-0.90$  V and  $-0.75$  V,

respectively, and at the negative end of the CV scan, nearly twice as much methane is detected than ethylene. Figure 1D shows that polycrystalline copper and CuCube have similar onsets for hydrogen formation, but the CuCube sample produces more hydrogen overall, which is consistent with the fact that also more overall current is drawn on the CuCube sample. The onset for methane production on the two samples is also very similar (albeit the intensity for methane production on CuCubes is almost negligible), but their onset for and selectivity toward ethylene is very different. CuCube has an onset of  $-0.6$  for ethylene formation (vertical dashed line), which is more positive than the polycrystalline sample, and also produces a relatively large amount of ethylene across the voltage range measured. In fact, with nearly complete suppression of the methane signal, the selectivity for the CuCube sample toward ethylene has increased by more than two orders of magnitude compared to polycrystalline copper.

To better understand the dramatic increase in the ethylene to methane selectivity of the CuCube sample, the CO<sub>2</sub>RR activity of three different copper single-crystal surfaces, Cu(111), Cu(211), and Cu(100), was studied in the same setup. The cubic structure present on the CuCube sample suggests the surface is dominated by the (100) facet of copper and (100) step sites. By comparing the activity of the single crystals to the CuCube surface, we can begin to understand what leads to its high activity.

Figure 2 shows the results for the single-crystal experiments with Figure 2A displaying the CVs for the three

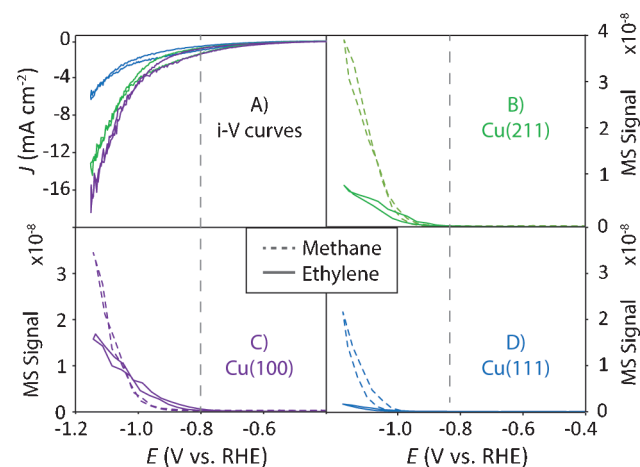


**Figure 2.** A) Comparison of single-crystal CVs in  $0.1$  M KHCO<sub>3</sub>. Methane and ethylene formation on B) Cu(211), C) Cu(100), and D) Cu(111).

surfaces and Figure 2B–D showing the ethylene and methane products of the (211), (100), and (111) orientations, respectively. Both the forward and reverse scans are plotted for the ethylene and methane product channels and show very little hysteresis. All three surfaces make both ethylene and methane, and a qualitative interpretation of the results shows the Cu(111) surface being the least active (it also pulls the least amount of current) whereas the Cu(100) and Cu(211) appear fairly similar in activity. Upon closer exami-

nation it becomes clear that the Cu(100) has a higher selectivity for ethylene at lower overpotential (vertical dashed line in Figure 2) and there is in fact a range of potentials on the Cu(100) surface at which a significant amount of ethylene is produced and methane is not (−0.8 to −1.0 V).

Table 1 summarizes the ethylene onset potentials for the different surfaces investigated and they are arranged in order

**Table 1:** Onset potentials (V vs. RHE) for ethylene and methane production from reducing CO<sub>2</sub> in 0.1 M KHCO<sub>3</sub>. The copper surfaces are listed in order of ethylene onset.

Surface	C <sub>2</sub> H <sub>4</sub> onset potential	CH <sub>4</sub> onset potential
Cu(Cube)	−0.60 V	−0.93 V
Cu(100)	−0.73 V	−0.90 V
Cu(Poly)	−0.74 V	−0.95 V
Cu(211)	−0.79 V	−0.94 V
Cu(111)	−0.96 V	−0.99 V

of best to worst in terms of ethylene selectivity with CuCube being far and away the best surface investigated. When comparing the single crystals, Cu(100) has the most favorable selectivity for ethylene production and the earliest onset potential. Cu(211), which has (100) step sites, is the next best in terms of ethylene selectivity, with Cu(111) being the worst surface studied. The single-crystal study suggests that this cubic surface structure is preferable for ethylene selectivity compared to the close-packed (111) surface or the highly stepped (211) surface.

What the single-crystal studies fail to explain, however, is the complete lack of methane formation on the CuCube sample. Whereas the (100) surface is the most comparable to the CuCube surface in terms of ethylene onset potential, the (100) surface still makes a significant amount of methane. The (211) surface, which has two-atom-wide terraces and (100) steps, also produces significant amounts of methane and is less selective for ethylene. Work performed by Hori et al.<sup>[8]</sup> on single-crystal surfaces suggest there is an ideal terrace length that gives the maximum ethylene to methane ratio with the (100), largely devoid of steps, and the (211), having the highest step density, the two extremes that give the smallest ethylene to methane ratio. Hori found the Cu(711) surface to be the most selective for ethylene, giving an ethylene to methane ratio of 10:1. Due to the high selectivity of the CuCubes, it is reasonable to conclude that the CuCube surface either has a very high density of ethylene-selective active sites compared to other CO<sub>2</sub>RR catalysts studied, or it presents a new active site not found on other surfaces.

Another possibility that cannot be ruled out at this point is that due to the rough nature of the CuCube surface, the local pH during reaction is much higher than the bulk pH, and it is this rise in local pH that improves the selectivity of the CuCube surface. Previous work has demonstrated the importance of pH (bulk) on CO reduction over copper electrodes, especially showing an earlier onset potential for ethylene at higher pH.<sup>[4b,d]</sup> Similarly, local pH changes (not just bulk changes) can affect the selectivity of copper electrodes, and

recent reports estimate that at typical current densities and electrolyte concentrations, the local pH in a neutral bulk solution of KHCO<sub>3</sub> can be as high as 10–11.<sup>[9]</sup> Given these results for an electrode roughness factor of 16, and the fact that we estimate the CuCubes roughness factor to be about 20, it is reasonable to assume that the local pH during the CO<sub>2</sub>RR over CuCubes is also somewhere around 10.5 which could shift, somewhat, the selectivity toward ethylene. This difference in local pH versus bulk pH is only thought to be present on rough surfaces, and absent from single-crystal surfaces, possibly contributing to the disconnect we see between the CuCube and Cu(100) selectivities.

The CuCube electrocatalyst presented here is one of the most selective for ethylene over methane, implying that it favors C–C coupling to make multicarbon products instead of completely reducing a single carbon to methane. The ability to catalyze ethylene formation without significant methane production indicates that these two products are most likely formed through two distinct, competing pathways (see SI for more discussion). Finding a surface that favors the C–C coupling pathway (such as the CuCube surface reported here) is important for ultimately controlling the selectivity of the CO<sub>2</sub>RR for multicarbon product formation.

## Experimental Section

Polycrystalline copper disks with dimensions of 8 mm diameter, 2.5 mm high were machined from OHFC copper of 99.9% purity. Copper single crystals of the same dimensions were purchased from Princeton Scientific and are polished to an accuracy of <0.1 degree with a roughness <0.01 micron (99.9999% pure). Copper working electrodes were prepared by electropolishing in 85% phosphoric acid at 2 V for 60 seconds (polycrystalline electrodes) or 20 seconds (single-crystal electrodes). The electrodes were then directly submerged in an aqueous electrolyte solution of 0.1 M KHCO<sub>3</sub> purged with CO<sub>2</sub>. The resulting electrolyte pH was 6.8. Cyclic voltammograms (CVs) were measured using an Ag/AgCl reference electrode (Accumet), a boron doped diamond counter electrode (CCL Diamond), and a Biologic VSP 200 potentiostat scanning at a rate of 5 mVs<sup>−1</sup>. The solution resistance was determined by electrochemical impedance spectroscopy measured after each CV at 10 kHz and the potentiostat was set to compensate for 85% of the measured IR drop. CuCube electrodes were prepared in situ by adding 4 mM KCl to the standard 0.1 M KHCO<sub>3</sub> electrolyte and cycling the potential of an electropolished polycrystalline copper disk between −1.15 V and 0.9 V at 5 mVs<sup>−1</sup> for three cycles until a stable CV was achieved. Copper electrode surfaces were characterized by X-ray photoelectron spectroscopy (XPS, PHI Versaprobe), X-ray diffraction (XRD, Panalytic X'Pert 1), and scanning electron microscopy (SEM, FEI XL30 Sirion). Capacitive scans (Figure S6) were used to estimate the roughness factor of the CuCube electrode to around 20.

Online electrochemical mass spectrometry (OLEMS) was used to detect the CO<sub>2</sub>RR products formed during each CV. The setup was adapted from Koper et al.<sup>[10]</sup> and consisted of a mass spectrometer (SRS CIS 300) measuring electrochemical reaction products that enter the system through a porous Teflon frit (Porex 15–25 μm) placed near the surface of the copper working electrode. Details of the setup are shown in Figure S2. The principal improvement over the previously reported system, was the use of custom copper disk holder. This allowed the face of the working electrode to be placed vertically, so that bubbles formed at high current density could escape from the surface. Trapped bubbles can interfere with the mass transport of CO<sub>2</sub>

to the surface and contribute to noise in the potentiostat and mass spectrometer readings.

**Keywords:** carbon dioxide · electrocatalysis · electrochemical reduction · nanomaterials

**How to cite:** *Angew. Chem. Int. Ed.* **2015**, *54*, 5179–5182  
*Angew. Chem.* **2015**, *127*, 5268–5271

- 
- [1] a) G. A. Olah, G. K. S. Prakash, A. Goepfert, *J. Am. Chem. Soc.* **2011**, *133*, 12881–12898; b) N. S. Lewis, D. G. Nocera, *Proc. Natl. Acad. Sci. USA* **2006**, *103*, 15729–15735.
- [2] a) Y. Hori, *Handbook of Fuel Cells: Fundamentals, Technology and Application*, Vol. 2 (Eds.: A. L. W. Vielstich, H. A. Gasteiger), John Wiley & Sons, Weinheim, **2003**, pp. 720–733; b) A. A. Peterson, F. Abild-Pedersen, F. Studt, J. Rossmeisl, J. K. Nørskov, *Energy Environ. Sci.* **2010**, *3*, 1311–1315; c) K. P. Kuhl, E. R. Cave, D. N. Abram, T. F. Jaramillo, *Energy Environ. Sci.* **2012**, *5*, 7050–7059; d) K. Manthiram, B. J. Beberwyck, A. P. Alivisatos, *J. Am. Chem. Soc.* **2014**, *136*, 13319–13325.
- [3] C. W. Li, M. W. Kanan, *J. Am. Chem. Soc.* **2012**, *134*, 7231–7234.
- [4] a) K. J. P. Schouten, Y. Kwon, C. J. M. van der Ham, Z. Qin, M. T. M. Koper, *Chem. Sci.* **2011**, *2*, 1902–1909; b) K. J. P. Schouten, E. Pérez Gallent, M. T. M. Koper, *J. Electroanal. Chem.* **2014**, *716*, 53–57; c) K. J. P. Schouten, E. Pérez Gallent, M. T. M. Koper, *ACS Catal.* **2013**, *3*, 1292–1295; d) K. J. Schouten, Z. Qin, E. Pérez Gallent, M. T. Koper, *J. Am. Chem. Soc.* **2012**, *134*, 9864–9867.
- [5] a) C. S. Chen, A. D. Handoko, J. H. Wan, L. Ma, D. Ren, B. S. Yeo, *Catal. Sci. Technol.* **2015**, *5*, 161–168; b) J. Bugayong, G. L. Griffin, *ECS Trans.* **2013**, *58*, 81–89.
- [6] G. Bianchi, P. Longhi, *Corros. Sci.* **1973**, *13*, 853–864.
- [7] H. Liu, Y. Zhou, S. A. Kulinich, J.-J. Li, L.-L. Han, S.-Z. Qiao, X.-W. Du, *J. Mater. Chem. A* **2013**, *1*, 302.
- [8] Y. Hori, I. Takahashi, O. Koga, N. Hoshi, *J. Mol. Catal. A* **2003**, *199*, 39–47.
- [9] R. Kas, R. Kortlever, A. Milbrat, M. T. Koper, G. Mul, J. Baltrusaitis, *Phys. Chem. Chem. Phys.* **2014**, *16*, 12194–12201.
- [10] A. H. Wonders, T. H. M. Housmans, V. Rosca, M. T. M. Koper, *J. Appl. Electrochem.* **2006**, *36*, 1215–1221.

Received: December 19, 2014

Revised: February 2, 2015

Published online: February 26, 2015